Eur Biophys J (2010) 39:711–719
DOI 10.1007/s00249-009-0565-3

ORIGINAL PAPER

Distance and dynamics determination by W-band DEER and W-band ST-EPR

Likai Song · Mioara Larion · Jean Chamoun · Marco Bonora · Piotr G. Fajer

Received: 27 May 2009 / Revised: 30 July 2009 / Accepted: 12 November 2009 / Published online: 9 December 2009

Abstract To explore high-field EPR in biological applications we have compared measurements of dynamics with X-band (9 GHz) and W-band (94 GHz) saturation transfer EPR (ST-EPR) and distance determination by X and W-band DEER. A fourfold increase of sensitivity was observed for W-band ST-EPR compared with X-band. The distance measurements at both fields showed very good agreement in both the average distances and in the distance distributions. Multifrequency EPR thus provides an additional experimental dimension to facilitate extraction of distance populations. However, the expected orientational selectivity of W-band DEER to determine the relative orientation of spins has not been realized, most likely because of the large orientational disorder of spin labels on the protein surface.

Keywords EPR · W-band · ST-EPR · DEER

Abbreviations

cdb3	Cytoplasmic domain of band 3
CW EPR	Continuous wave electron paramagnetic resonance
DEER	Double electron electron resonance
ELDOR	Electron–electron double resonance
EPR	Electron paramagnetic resonance
MSL	*N*-(1-oxy-2,2,5,5-Tetramethyl-4-piperidinyl)maleimide
MTSSL	1-Oxyl-2,2,5,5-tertramethyl-Delta^3-pyrroline-3-(methyl)methanethisulfonate
SDSL	Site-directed spin labelling
ST-EPR	Saturation transfer electron paramagnetic resonance
T4L	T4 lysozyme
Tn	Troponin
TnC	Troponin C

The more you see: spectroscopy in molecular biophysics.

L. Song · M. Larion · J. Chamoun · M. Bonora · P. G. Fajer (✉)
National High Magnetic Field Laboratory, Institute of Molecular Biophysics, Department of Biological Science, Department of Biochemistry and Chemistry, Florida State University, Tallahassee, FL 32310, USA
e-mail: fajer@magnet.fsu.edu

Introduction

Electron paramagnetic resonance (EPR) spectroscopy is a powerful tool used in structural biology to determine protein structure, dynamics, conformational changes, and relative orientation of protein components. EPR spectra depend strongly on the interplay of magnetic field-dependent and magnetic field-independent interactions. By operating at low field and 10-times higher field, we are able to resolve the contributions from the two types of interactions. Here, we compared the sensitivity of two popular EPR techniques conducted with the X-band (9.7 GHz) and the W-band (94.2 GHz). The two techniques are:

1 double electron electron resonance (DEER) for spin–spin distance measurements; and
2 saturation transfer EPR (ST-EPR) for rotational molecular motion determination.

DEER

The recent resurgence of EPR in structural biology is in large part because of the development of pulsed EPR

techniques and their application to biological systems, especially distance measurements by DEER. DEER, also known as pulsed electron–electron resonance (PELDOR), was initially proposed by Milov, Tsvetkov, and collaborators (Milov et al. 1981, 1984 and 1998).

The availability of commercial instrumentation and the ability to place labels at will via site-directed spin labelling has led to increased appreciation of the method, which was widely adopted because of the ground-breaking work of Jeschke and his group. A dead-time-free variant of the method, four-pulse DEER, is now a standard in the field (Pannier et al. 2000). More recently, several studies demonstrated that DEER techniques can be used at high fields (Denysenkov et al. 2006; Polyhach et al. 2007; Savitsky et al. 2007), which clearly gives an advantage of orientational selection for some samples. Here, we report the results of DEER measurements performed on five different protein samples with the X-band and the W-band.

Nitroxide–nitroxide distance measurements using a four-pulse DEER sequence is illustrated in Fig. 1, (Pannier et al. 2000). A spin echo (Hahn echo) is created by a two-pulse sequence at an observation microwave frequency ν_{observe} selecting only molecules with given orientation to the magnetic field. A pump pulse at a second microwave frequency ν_{pump} is inserted between the 2nd and 3rd pulses at a variable delay time t. As the delay time is swept between the observation pulses, the intensity of the echo is modulated, because of dipolar interactions between the spins resonating at ν_{observe} and spins resonating at ν_{pump} (Fig. 1).

The echo intensity oscillates with:

$$I_{\text{intra}}(t) = I_{\text{o}} \cos(\omega_{\text{AB}}(\tau - t)) \quad (1)$$

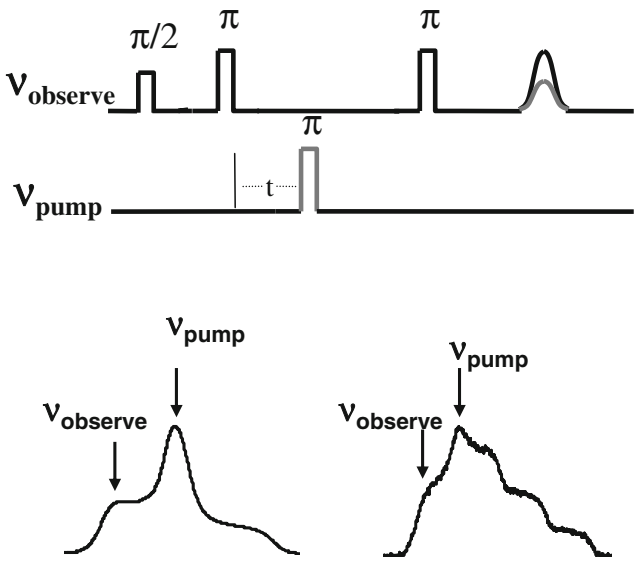

Fig. 1 Four-pulse DEER sequence and the "observe" and "pump" field positions for the X-band (*left*) and the W-band (*right*)

where I_{o} is the echo in the absence of dipolar interactions, τ is the time between the $\pi/2$ and π pulses, and t is the timing of the pumping pulse (Milov et al. 1981, 1984 and 1998).

Dipolar splitting, ω_{AB} between the two spins at a distance r is given by:

$$\omega_{\text{AB}} = \frac{\beta^2 g_{\text{A}} g_{\text{B}}}{\hbar r^3}(3\cos^2\theta_{\text{dd}} - 1) \quad (2)$$

in which the interspin vector subtends an angle θ_{dd} with an external magnetic field, β is the Bohr magneton, $\hbar$ is the Planck's constant, g_{A} and g_{B} are the effective g tensor of the coupled spins.

According to Eqs. 1 and 2, the DEER signal depends on the inter-spin distance (r), and the orientation of the spin–spin vector relative to the field (θ_{dd}). For reasons of sensitivity and of experimental convenience we often determine the inter-spin distances from a sample with randomly distributed angle θ_{dd}. However, the dependence of DEER signal on angle θ_{dd} is potentially beneficial for structural biology. For orientation-fixed spin pairs on a macromolecule, excitation of a set of orientations of the two spins will select a distinct inter-spin vector angle θ_{dd}. The dependence of DEER signal on the orientation enables determination of the mutual orientation of spin labels in the macromolecule. This requires "pumping" and "observing" spins at distinct orientational distributions which is easier to achieve with the W-band than with the X-band because of higher orientational dispersion.

ST-EPR

ST-EPR, developed by Hyde and Thomas in 1972 is a nonlinear method that measures the transfer of saturation throughout a spectrum because of spectral diffusion. With the X-band, the method is sensitive to rotational correlation times in the microsecond to millisecond time range (conventional EPR is not sensitive on this timescale). The increase of the Larmor frequency increases orientational dispersion and thus increases spectral diffusion $\delta H_r/\delta\Omega$ (defined as a change of resonating field H_r with angle Ω), which determines the sensitivity of ST-EPR to molecular motion. The increased spectral diffusion should lead to larger transfer of saturation when motion is slower and thus extend the upper limit of sensitivity. Similar extension of sensitivity was observed in 35 GHz Q-band EPR (Johnson et al. 1982).

The objective of this study was to investigate the sensitivity of ST-EPR at higher microwave frequencies (W-band). For comparison with previous work with the X-band we use haemoglobin as a model, spherical protein diffusing isotropically according to the Stokes–Einstein equation:

$$\tau_c = 4\pi\lambda r^3/3\text{kT} \quad (3)$$

where λ is the medium viscosity, k is the Boltzmann constant and T is the absolute temperature. The radius of haemoglobin (r) is 29 Å (Jones and Johnson 1978). The rotational correlation times (τ_c) were varied from microsecond to millisecond timescales by varying the viscosity of glycerol–water mixtures. Haemoglobin was labelled with ^{15}N-MSL (^{15}N-(1-oxyl-2,2,6,6-tetramethyl-4-piperidinyl) maleimide), which provides increased spectral resolution compared with ^{14}N, by having only two nuclear manifolds instead of three.

Materials and methods

Proteins

Troponin C (*TnC*) cysteine mutant at positions 55 and 83 was expressed, purified, and spin labelled as previously described (Brown et al. 2002). *Erythrocyte cytoplasmic domain of band 3* (*cdb3*) mutants were expressed and spin labelled as described by Zhou et al. (2007). *T4 lysozyme* (*T4L*) double cysteine mutants T4L_21C65C and T4L_65C89C were expressed in *Escherichia coli* K38 cells (McHaourab et al. 1996). All above samples for DEER measurements were labelled with MTSSL ((1-oxyl-2,2,5,5-tetramethyl-Δ^3-pyrroline-3-methyl)methanethiosulfonate). *Haemoglobin* was isolated from red blood cells. Purified haemoglobin was labelled with ^{15}N-MSL (^{15}N-(1-oxyl-2,2,6,6-tetramethyl-4-piperidinyl) maleimide). EPR samples were prepared by diluting concentrated labelled haemoglobin with glycerol–water mixtures to a final haemoglobin concentration of approximate 1 mM. Solvent viscosities were previously measured by Fajer and Marsh (1983).

DEER measurements

The DEER experiments were performed on a Bruker E680 X/W-band pulsed EPR instrument (Bruker Spectrospin, Billerica, MA, USA), at 65 K. X-band DEER was carried out using a 16-ns 90° pulse in an overcoupled dielectric resonator (Bruker, ER 4118X-MD5), with a 32-ns, 180° ELDOR pulse at $\sim$70 MHz below the observation frequency (Fig. 1). W-band DEER was carried out in a Bruker cylindrical cavity (Bruker E-600–1021 HE) with a 32-ns 90° observing pulse and a 64-ns 180° ELDOR pulse at $\sim$70 MHz below the observation frequency (Fig. 1). Spin-labelled protein samples with a spin label concentration ranging from 80 to 200 μM were used for DEER measurements. The sample volumes were 100 μl for the X-band and 1 μl for the W-band. For frequency separation sweep measurement, the ELDOR frequency was kept at the centre of the W-band spectrum, while the "observed" spins were selected at different positions ±30 Gauss from the pumped position. The frequency difference between "pumped" and "observed" spins is limited by the 200-MHz bandwidth of the relatively high Q ($\sim$1,000) cavity.

DEER spectra simulation and data analysis

The distribution of distances from DEER spectra was obtained by fitting calculated dipolar evolution spectra corresponding to Gaussian distribution of distances to experimental DEER spectra. The DEER signal for a Gaussian distribution of distances centred at r_o and with halfwidth of Δr, $\Gamma(r) = A\exp\left(-0.693\frac{(r-r_o)^2}{\Delta r^2}\right)$ is simulated by:

$$I_{\text{intra}}(t,r) = \int_r \Gamma(r) \int_0^{\pi/2} I_0 \sin\theta_{\text{dd}} \cos \times \left(\frac{\beta^2 g_A g_B}{\hbar r^3}\left(3\cos^2\theta_{\text{dd}} - 1\right)(\tau - t)\right) \mathrm{d}\theta_{\text{dd}}\mathrm{d}r \quad (4)$$

where I_o is the echo in the absence of dipolar interactions, τ is the time between the $\pi/2$ and π pulses, and t is the timing of the pumping pulse. θ_{dd} is the angle the interspin vector subtends in an external magnetic field, and g_A and g_B are the g tensors of the coupled spins. The simulated spectrum is then compared with the experimental spectrum until a satisfactory fit is obtained. The number of Gaussian populations was determined by *f*-test as described in (Fajer et al. 2007).

Simulation of "Pake" pattern for partially disordered spins

For partially disordered spin pairs on a macromolecule, limited excitation/pumping of a subset of orientations selects a distinct set of inter-spin vector angles θ_{dd}, which results in a distorted Pake pattern. For different observation and pumping pulse positions, we first determine the orientational distributions of the two spin populations. At any field position, H_{res}, the resonating spins have to satisfy Eq. 5:

$$H_{res}(\theta,\phi,m_1) = \frac{h\nu}{\beta g(\theta,\phi)} + m_1 A(\theta,\phi) \quad (5)$$

where m_1 is the nuclear spin quantum number, h is Planck's constant, and ν is the microwave frequency. Here, the g and hyperfine splitting A tensors of the spins are determined by the spin orientation (θ, ϕ) with respect to the static magnetic field:

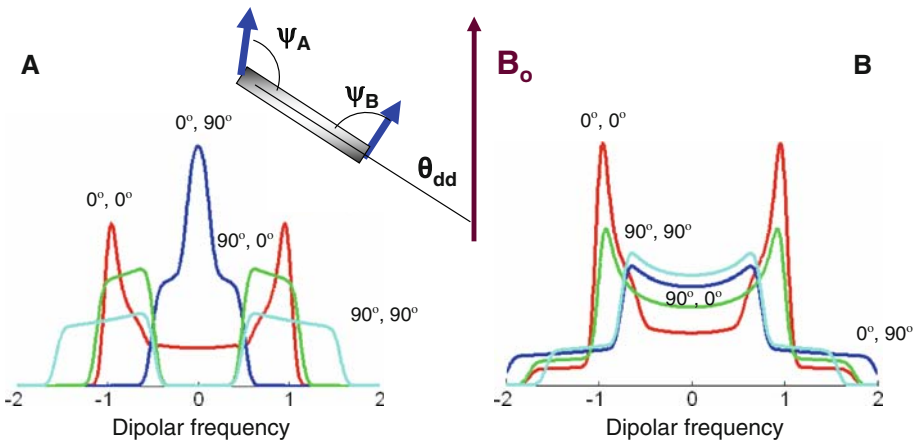

Fig. 2 Dipolar frequency patterns predicted for (**a**) the low-field region (g_x) and (**b**) the center of the spectrum (g_y) for four models of different spin orientation with respect to the interspin vector (ψ_A, ψ_B) of (0°, 0°), (0°,90°), (90°,0°), and (90°,90°). Each of the spins was disordered by ±22° in ψ_A, and ψ_B

$$g(\theta,\phi) = g_{xx}\sin^2\theta\cos^2\phi + g_{yy}\sin^2\theta\sin^2\phi + g_{zz}\cos^2\theta \tag{6}$$

$$A^2(\theta,\phi) = A_{xx}^2\sin^2\theta\cos^2\phi + A_{yy}^2\sin^2\theta\sin^2\phi + A_{zz}^2\cos^2\theta \tag{7}$$

From the Eqs. 5–7 the relative orientation of the two spin populations determines the inter-spin vector angles θ_{dd}. For completely disordered spins (disorder in the interspin angle) the orientation of the resonating populations does not predetermine the orientation of the spin–spin vector with respect to the field, θ_{dd}, and the dipolar interaction is calculated by integration of the field splitting over the angle θ_{dd}, Pake pattern—Pake(H, r). The integral is convoluted with a resonance absorption line (width $\Delta\Gamma = 3$G for frozen protonated nitroxide) at the resonance field corresponding to the angle θ_{dd}.

$$\mathrm{Pake}(H,r) = \int_0^{\pi/2} \sin(\theta_{dd})\exp\left(-0.693\frac{(H-D(r))^2}{\Delta\Gamma^2}\right)d\theta_{dd} \tag{8}$$

where:

$$D(r) = \pm\frac{3g\beta(3\cos^2\theta_{dd}-1)}{4r^3} \tag{9}$$

For perfectly ordered spins selection of the pumped and observed spins determines the spin–spin orientation with respect to the external field. This depends on the physical arrangement of the spin axes and their inter-spin vectors. We have considered four limiting cases, magnetic tensors colinear with the interspin vector; observed spins parallel to the interspin vector—pumped spin perpendicular; observed spins perpendicular to the interspin vector which is parallel to the pumped spin, and the arrangement where pumped, observed spin, and interspin vector are all mutually perpendicular. Each of these limiting cases was then modified to allow for arbitrary disorder of the observed and pumped spin with respect to the interspin vector (Fig. 2).

ST-EPR and power saturation measurements

We have followed the standard procedure proposed by Hemminga et al. (1984). X-band ST-EPR experiments were performed using Bruker dielectric cavity for the X-band and the TE011 cavity for the W-band. Second harmonic out-of-phase signals, V_2', were recorded at the same fractional saturation for the X and W-bands: 32 mW incident power for the X-band and 4 mW for the W-band. For X-band measurements, samples were placed in 0.9 mm i.d. glass capillaries (VWR); for the W-band, samples were placed in a quartz fused capillary of 0.15 mm i.d. (Vitrocom) and placed in a larger 0.5 mm i.d. capillary (Bruker). The sample volumes were 25 and 0.2 μL for X-band and W-band, respectively. The scan widths were 160 and 250 G (for the X and W-bands, respectively), the time constants 40 and 81 ms, the conversion times 40 and 81 ms, and the averaging times 15 min and 1 h; the modulation amplitude was five Gauss. The phase was also monitored before and after the data collection and corrected if necessary.

Results and discussion

DEER

Comparison of X-band and W-band DEER

To compare the DEER for the X-band and the W-band, the spectra of five doubly spin-labelled mutants from three different proteins, T4L, TnC, and cdb3, were collected with a four-pulse DEER sequence (Fig. 1). T_2 relaxation times

differed by 10% between the two frequencies (3.5 μs at X- and 3.2 μs at W-band). It is immediately obvious that the DEER spectra were similar for X and W-bands for all five samples (Fig. 3). Quantitative analysis of the DEER spectra was performed by fitting calculated dipolar evolution spectra corresponding to a set of Gaussian distributions. The recovered distance populations were in good agreement between the two frequencies, Table 1.

The main rationale for multifrequency DEER is orientational selectivity. However, comparison of the two frequencies is of value in itself: it provides an independent check whether or not the orientational effects are present at either frequency, and adds an independent experimental data set to what is generally recognized as an ill-determined problem.

Orientational selectivity of W-band DEER

The orientation-selective feature of DEER measurements potentially allows determination of mutual orientation of spin labels in macromolecules. Larsen and Singel showed theoretically that the observed dipolar frequency should be correlated with the pumping/observe positions (Larsen and Singel 1993). This is difficult to accomplish with the X-band, with which spectral dispersion is small, but the development of commercial high-field spectrometers (Bruker) enables exploration of this possibility at higher fields. Orientation-dependent DEER has been observed for well defined model systems, bi and triradicals (Polyhach et al. 2007), and for tyrosyl radicals in ribonucleotide reductase (Denysenkov et al. 2006).

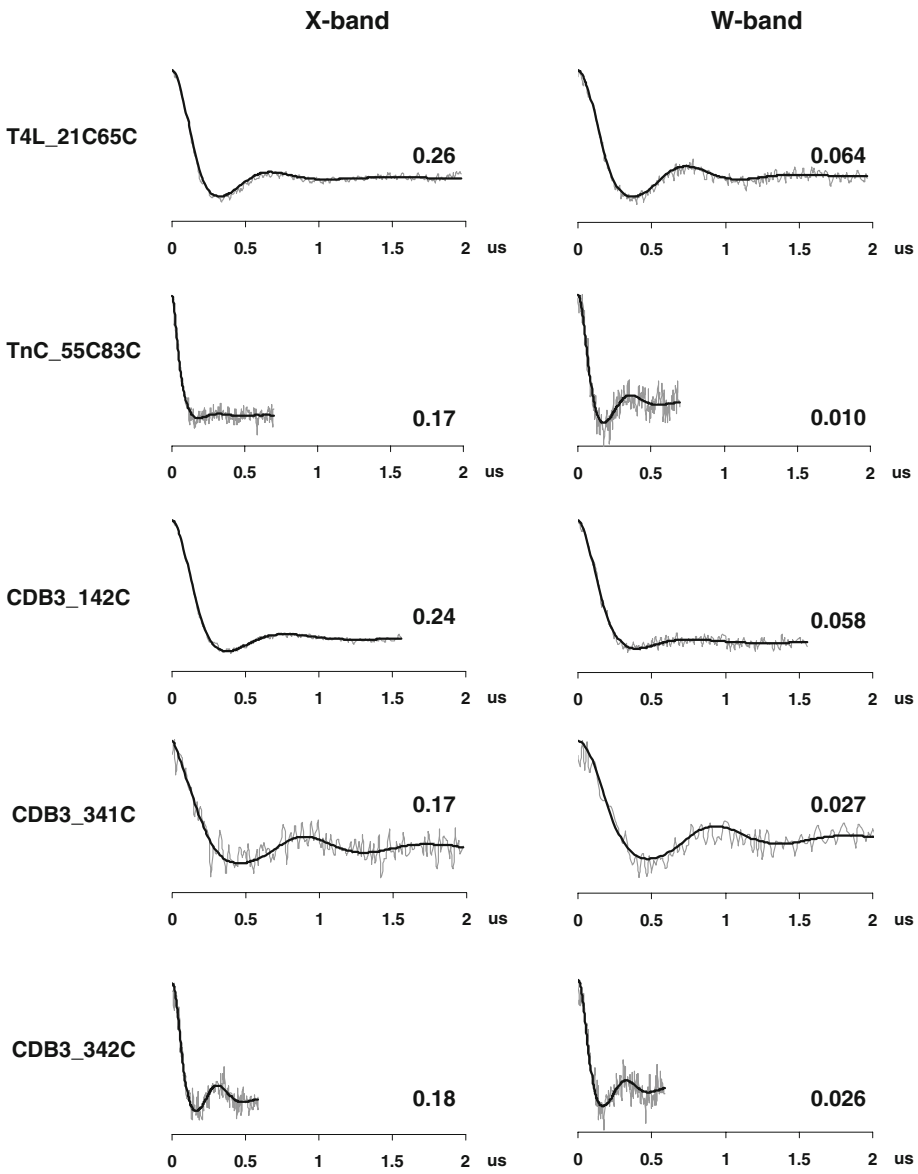

Fig. 3 Comparison of X-band and W-band DEER for T4 lysozyme (T4L_21C65C), troponin C (TnC_55C83C), and the cytoplasmic domain of Band 3 protein (CDB3_142C, 341C and 342C). Intensity normalized DEER evolution curves are shown for comparison. The modulation depth values are indicated on the *right* of the spectra. The "pump" and "observe" pulse positions are as shown in Fig. 1

Table 1 Comparison of distance distributions for the X-band and the W-band

Sample	X-band		W-band	
	Average distance (Å)	Distance distribution (Å)	Average distance (Å)	Distance distribution (Å)
T4L_21C65C	31 ± 1	6 ± 2	32 ± 1	5 ± 2
TnC_55C83C	24 ± 2	11 ± 5	25 ± 2	6 ± 5
CDB3_142C	32 ± 1	7 ± 2	33 ± 2	10 ± 3
CDB3_341C	33 ± 3	8 ± 6	35 ± 2	4 ± 3
CDB3_342C	25 ± 1	3 ± 2	25 ± 2	3 ± 2

In order to look for orientation-dependent DEER in typical protein systems we performed a frequency separation sweep experiment with varied observation pulse frequencies. The pumping frequency selects always the same population of spins at the centre of the spectrum. The pumped spins subtend the orientational range of $\theta = 40$–$90°$ while the observed spins orientation varies from $\theta = 64$–$90°$ for the downfield region to $\theta = 0$–$19°$ and 35–68° for the upfield region (Fig. 4, lower panel). Compared with the centre of the W-band spectrum, the downfield region is especially discriminating for orientational effects in the spectrum. The simulated frequency distribution for four different simple models of the relative orientation of the spin tensors with respect to the interspin vector (ψ_A, ψ_B) clearly do not result in a Pake pattern (Fig. 2a). In this region, the difference between the Pake pattern and the predicted population persists even in the presence of large disorder of the spin with regard to the interspin vector, for 22° disorder only one model (both spins are parallel to the interspin vector, ψ_A, $\psi_B = 0°$) resembles a Pake pattern. At the centre of the W-band spectrum this difference vanishes more quickly; for the same disorder the simulated distributions resemble Pake patterns, albeit distorted in their singularities (Fig. 2b). Thus comparison of the DEER signals at these fields should be most sensitive to orientational selection. Yet, the experimental DEER spectra from T4L_65C89C shown in Fig. 4 show little if any variation. Quantitative analysis revealed that all the spectra can be accounted for by a population of $r_{av} = 30 \pm 2$ Å and a distance spread of $\Delta r = 6 \pm 3$ Å.

The absence of an orientational effect can be because of a number of reasons:

– instrumental: for example variation of the relative strength of pump/observe pulses when varying their separation; and
– sample considerations: disorder in the relative orientation of pumped and observed spins and even the orientation of the spin labels with respect to the interspin vector connecting them.

To avoid these problems we have chosen a sample of a coiled-coil protein, tropomyosin, for which the orientation of spin with regard to the long axis of the protein is known,

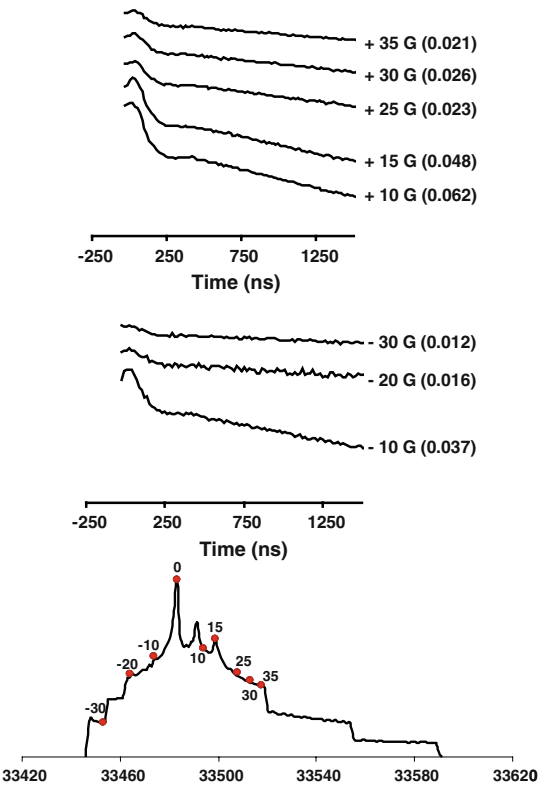

Fig. 4 W-band DEER spectra of T4L_65C89C, with a "pump" position at the maximum of the spectrum and varying "observe" positions (*bottom*). The modulation depth values are indicated in *parentheses*

as also is the orientation of the interspin vector (it is parallel dimer, ψ_A, $\psi_B = 90°$). To limit the variation in the pump and observe frequency pulses, the offset between the two is kept at 30 MHz, and different positions in the spectrum are scanned. This method allows sufficient microwave power for both pulses and avoids the bandwidth limitation of the resonator. For most of the models the spectra in the low field (g_x) position are predicted to result in the largest orientational dependence when compared with the spectra in the g_y region (Fig. 2). As before, disappointingly, very little difference is observed (*data not shown*). Simulations suggest that around 45° disorder of each of the spins with regard to interspin vector obliterates

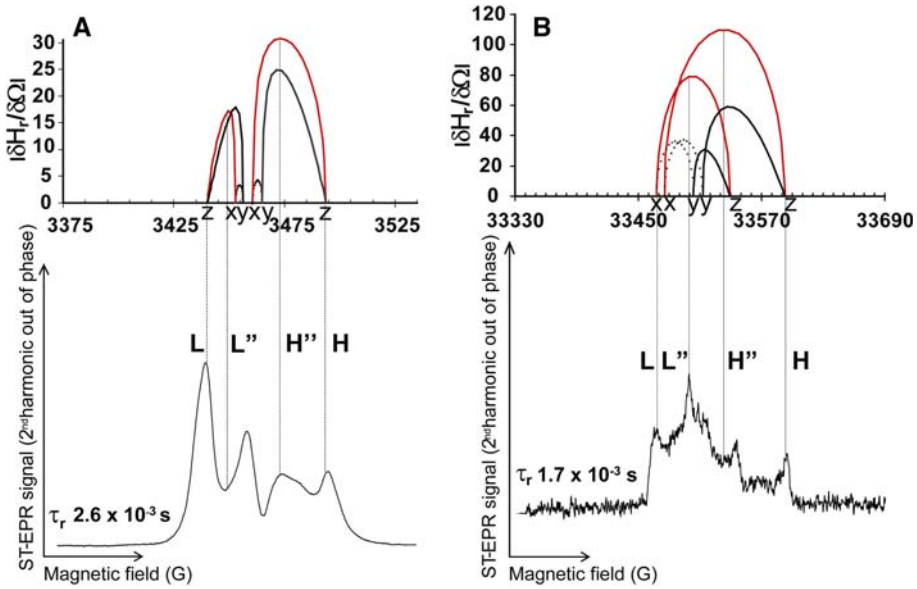

Fig. 5 Spectral diffusion $\delta H_r/\delta\Omega$ for the X-band (**a**) and the W-band (**b**). Maximum sensitivity to motion predicted by $\delta H_r/\delta\Omega$ calculations are labelled L″ for the 1/2 nuclear manifold and H″ for the −1/2 nuclear manifold. L″ and H″ provide sensitivity to the rate at which molecular motion is sweeping the nitroxide z axis into the x axis. Sensitivity to θ denoted by *grey lines*, sensitivity to φ by *black lines*

the distortions of the Pake pattern. For such samples, which might well be the case here, orientational selectivity will not be observed.

A conservative conclusion is that orientationally dependent DEER will be limited to samples where the orientation of the spin label is very well defined (disorder <22°), the spin labels should not be parallel to the interspin vector. To observe deviations from the Pake pattern, the stability and the sensitivity of the W-band instrument will be crucial. The DEER experiments with the W-band took a factor of ten longer than those with the X-band, possibly reflecting a smaller number of pumped spins because of limited strength of the pumping pulse and lower sensitivity of the commercial instrument operating at 95 GHz.

ST-EPR with the X and W-bands

ST-EPR experiments are conducted under partial saturation. The response of the system—transfer of saturation due to spectral diffusion induced by rotational motion—is a function of the saturation level itself (Fajer and Marsh 1983; Squier and Thomas 1986). The accepted standard conditions of $\langle H_1^2 \rangle_s = (0.25)^2\ G^2$ over the sample (Hemminga et al. 1984) are calibrated using PADS as a standard. Because the microwave source for the W-band is limited to 4 mW we have compared the X and W-band spectra at the same value of saturation of 80% rather than the absolute value of magnetic field. The saturation values were determined from the power dependence of the V_1 signal at both frequencies.

The sensitivity of ST-EPR spectra to rotational diffusion is proportional to the change in the resonance field (H_r), as a function of spin label orientation; $\Omega = (\theta, \phi)$. θ, ϕ are the polar angles between the spin label and the external field

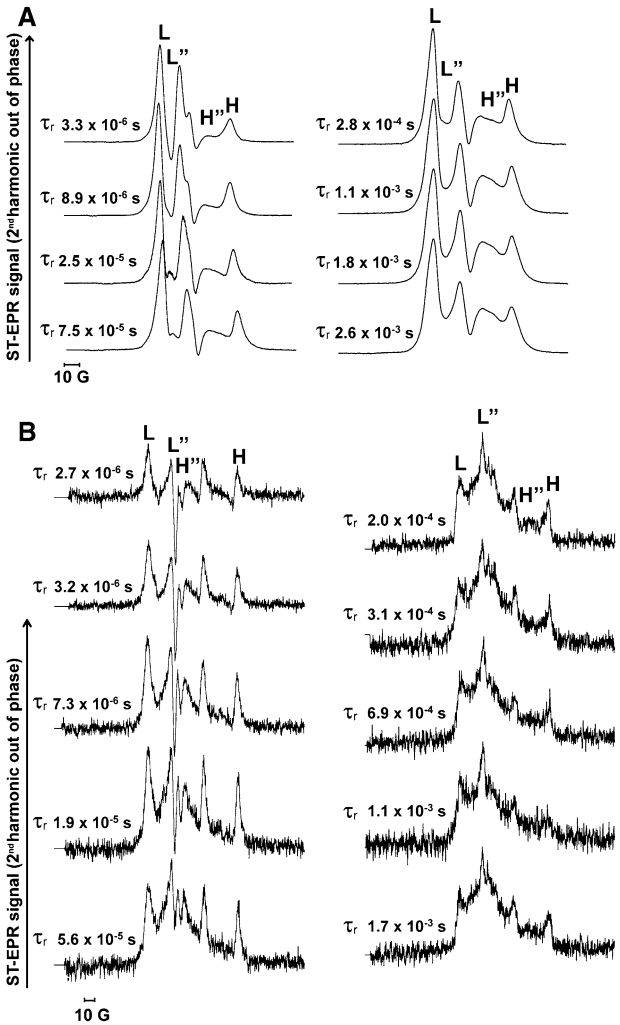

Fig. 6 The sensitivity of V2′ lineshapes to spectral diffusion of the labelled haemoglobin for the X-band (**a**) and the W-band (**b**)

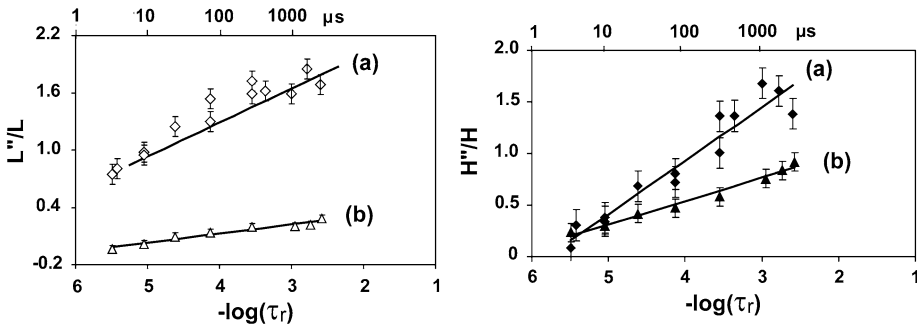

Fig. 7 The dependence of lineshape ratios on the rotational correlation times. L″/L (*left*) and H″/H (*right*): (*a*) W-band (*open and closed diamonds*); (*b*) X-band (*open and closed triangles*)

H_r is given by Eq. 5, and the effective g and A tensors are given by Eqs. 6 and 7. Differentiation gives angular sensitivity:

$$\Delta H_r/\delta\phi = \left[\frac{h\nu}{g^3\beta}\left(g_{zz}^2 - g_{xx}^2\cos^2\phi - g_{yy}^2\sin^2\phi\right) + \frac{m_i}{A}\left(A_{zz}^2 - A_{xx}^2\cos^2\phi - A_{yy}^2\sin^2\phi\right)\right]\sin\theta\cos\theta \quad (10)$$

$$\Delta H_r/\delta\phi = \left[\frac{h\nu}{g^3\beta}\left(g_{xx}^2 - g_{yy}^2\right) + \frac{m_i}{A}\left(A_{xx}^2 - A_{yy}^2\right)\sin\phi\cos\phi\sin^2\theta\right] \quad (11)$$

The plot of $\delta H_r/\delta\Omega$ versus field identifies the regions in the ST-EPR signal with varying motional sensitivity. x, y, z in Fig. 5 are the turning points for which the rate of change in H_r with respect to θ approaches 0. The maximum sensitivity is at intermediate positions. These positions are labelled L″ and H″, and for the X-band they correspond to the change of the hyperfine interactions as the *z*-axis is sweeping in the *xy*-plane; whereas for the W-band the same motion changes Zeeman interactions because of g-tensor anisotropy. The increased microwave frequency increases the spectral dispersion of the g-anisotropy which is 120 Gauss for the W-band compared with 35 Gauss hyperfine anisotropy for the X-band. This three to fourfold increase of the spectral dispersion is the basis for the increased sensitivity of W-band ST-EPR. At the L″ position the increase in $\delta H_r/\delta\Omega$ for the W-band compared with the X-band was 4.7-fold, and at H″ the increase was threefold.

Such increased sensitivity was predicted by spectral simulations by Hustedt and Beth (2004) and is borne out by the changes in the lineshapes of the experimental V2′ spectra (Fig. 6). As the correlation times increase from microsecond to millisecond the intensity at L″ and H″ is growing, but with a more pronounced increase for the W-band. The L″ and H″ intensities can be normalized to the intensities at the nearest turning points, because the latter are not affected by motion. These diagnostic lineheight ratios are plotted as a function of log(τ) in Fig. 7 for L″/L and H″/H. W-band L″/L values vary from 0.75 at correlation times of 3 µs to 1.85 for 1,640 µs correlation times compared with the X-band, for which L″/L values vary from −0.036 to 0.214 over the same timescale. If the sensitivity of the method is expressed in terms of the slope of diagnostic ratios then W-band ST-EPR is four times more sensitive than X-band ST-EPR for L″/L ratios and two times for H″/H values. This is in general agreement with the predicted increase of spectral diffusion of 4.7 and 3, respectively.

Acknowledgments Z. Zhou and Al Beth are thanked for the CDB3 samples, and H. McHaourab for the T4 lysozyme. This work was supported by an NSF MCB 0346650 grant to PF and the Elexsys 680 spectrometer was obtained through the NSF MRI grant to PF.

References

Brown LJ, Sale KL, Hills R, Rouviere C, Song L, Zhang X, Fajer PG (2002) Structure of the inhibitory region of troponin by site directed spin labeling electron paramagnetic resonance. Proc Natl Acad Sci USA 99:12765–12770

Denysenkov VP, Prisner TF, Stubbe J, Bennati M (2006) High-field pulsed electron-electron double resonance spectroscopy to determine the orientation of the tyrosyl radicals in ribonucleotide reductase. Proc Natl Acad Sci USA 103:13386–13390

Fajer PG, Marsh D (1983) Sensitivity of Saturation Transfer ESR Spectra to Anisotropic Rotation. Application to Membrane Systems. J Magn Reson 51:446–459

Fajer PG, Brown LJ, Song L (2007) Practical Pulsed Dipolar ESR (DEER). ESR Spectrosc Membr Biophy 27:95–128

Hemminga MA, de Jager PA, Marsh D, Fajer PG (1984) Standard conditions for the measurement of saturation-transfer ESR spectra. J Magn Reson 59:160–163

Hustedt EJ, Beth AH (2004) High field/high frequency saturation transfer electron paramagnetic resonance spectroscopy: increased sensitivity to very slow rotational motions. Biophys J 86:3940–3950

Hyde JS, Thomas DD (1973) New EPR methods for the study of very slow motion: application to spin-labeled hemoglobin. Ann NY Acad Sci 222:680–692

Johnson ME, Thiyagarajan P, Bates B, Currie BL (1982) A comparison of resolution-enhancement methods in saturation-transfer EPR. 15 N isotopically substituted spin labels and 35 GHz high-frequency operation. Biophys J 37:563–567

Jones CR, Johnson CS Jr (1978) Photon correlation spectroscopy of hemoglobin: diffusion of oxy-HbA and oxy-HbS. Biopolymers 17:1581–1593

Larsen RG, Singel DJ (1993) Double electron-electron resonance spin-echo modulation: spectroscopic measurement of electron spin pair separations in orientationally disordered solids. J Chem Phys 98:5134–5146

McHaourab HS, Lietzow MA, Hideg K, Hubbell WL (1996) Motion of spin-labeled side chains in T4 lysozyme. Correlation with protein structure and dynamics. Biochemistry 35:7692–7704

Milov A, Salikhov K, Shirov M (1981) Use of the double resonance in electron spin echo method for the study of paramagnetic center spatial distribution in solids. Fiz Tverd Tela (Leningrad) 23:957

Milov A, Ponomarev A, Tsvetkov Y (1984) Electron-electron double resonance in electron spin echo: model biradical systems and the sensitized photolysis of decalin. Chem Phys Lett 110:67

Milov AD, Maryasov AG, Tsvetkov YD (1998) Pulsed electron double resonance (PELDOR) and its applications in free-radical research. Appl Magn Reson 15:107–143

Pannier M, Veit S, Godt A, Jeschke G, Spiess HW (2000) Dead-time free measurement of dipole-dipole interactions between electron spins. J Magn Reson 142:331–340

Polyhach Y, Godt A, Bauer C, Jeschke G (2007) Spin pair geometry revealed by high-field DEER in the presence of conformational distributions. J Magn Reson 185:118–129

Savitsky A, Dubinskii AA, Flores M, Lubitz W, Mobius K (2007) Orientation-resolving pulsed electron dipolar high-field EPR spectroscopy on disordered solids: I. Structure of spin-correlated radical pairs in bacterial photosynthetic reaction centers. J Phys Chem B 111:6245–6262

Squier TC, Thomas DD (1986) Methodology for increased precision in saturation transfer electron paramagnetic resonance studies of rotational dynamics. Biophys J 49:921–935

Zhou Z, DeSensi SC, Stein RA, Brandon S, Song L, Cobb CE, Hustedt EJ, Beth AH (2007) Structure of the cytoplasmic domain of erythrocyte band 3 hereditary spherocytosis variant P327R: band 3 Tuscaloosa. Biochemistry 46:10248–10257